

# CAPABILITIES OF UV CORONAGRAPHIC SPECTROSCOPY FOR STUDYING THE SOURCE REGIONS OF SOLAR ENERGETIC PARTICLES AND THE SOLAR WIND

John L. Kohl, Steven R. Cranmer, Larry D. Gardner, Jun Lin, John C. Raymond, and Leonard Strachan

Harvard-Smithsonian Center for Astrophysics, Cambridge, MA 02138, USA

## ABSTRACT

We summarize the unique capabilities of UV coronagraphic spectroscopy for determining the detailed plasma properties (e.g., density, temperature, outflow speed, composition) of the source regions of both transient phenomena such as CMEs, flares, and solar energetic particles (SEPs) and more time-steady solar wind streams. UVCS/SOHO observations have provided the first detailed diagnostics of the physical conditions of CME plasma in the extended corona. It provided new insights into the roles of shock waves, reconnection, and magnetic helicity in CME eruptions. We summarize past observations and discuss the diagnostic potential of UV coronagraphic spectroscopy for characterizing two possible sites of SEP production: CME shocks and reconnection current sheets. UVCS/SOHO has also led to fundamentally new views of the acceleration region of the solar wind. Understanding the physical processes in this region, which ranges from the low corona ( $r = 1.1\text{--}1.5 R_{\odot}$ ) past the sonic points ( $r > 5 R_{\odot}$ ), is key to linking the results of solar imaging to *in situ* particle and field detection. Despite the advances that have resulted from UVCS/SOHO, more advanced instrumentation could determine properties of additional ions with a wider sampling of charge/mass combinations. This would provide much better constraints on the specific kinds of waves that are present as well as the specific collisionless damping modes. Electron temperatures and departures from Maxwellian velocity distributions could also be measured. The instrumentation capable of making the above observations will be described.

## 1. INTRODUCTION

In the following, we describe the capabilities of ultraviolet coronagraphic spectroscopy to address the SEP/flare/CME and solar wind problems, and we provide a brief description of a science payload that is capable of carrying out the required observations.

## 2. CMES, FLARES, AND SEPS

UVCS/SOHO observations have provided new insights into the roles of shock waves, reconnection, and magnetic helicity in CME eruptions (Raymond 2002).

### 2.1. CME Shocks

The key parameters in theories of particle acceleration by shocks are the pre-shock plasma conditions (including seed particle population), the shock speed, and the angle between the magnetic field and the shock motion.

UVCS has observed CME-driven shocks through their effect on the widths of UV spectral lines (Raymond et al. 2000; Mancuso et al. 2002). These observations provide information about the compression ratio in the shock, a crucial parameter for predicting SEP spectra, and information about the thermal equilibration among electrons, protons and heavier ions. Electron heating is relatively modest, and the line widths of oxygen and silicon ions imply temperatures far higher than the proton temperatures, a potentially important consideration for models of SEP composition. In some events, the shock compression ratio can be determined from Type II burst band splitting (e.g., Vršnak et al. 2002), but not all radio bursts contain enough detail for this diagnostic to be useful. For a much larger fraction of events, UV spectroscopy can be used to determine the compression ratio via two independent techniques: (1) measuring pre- to post-shock temperature ratios (i.e., both  $T_p$  and  $T_e$ ) with resonant and Thomson-scattered H I Ly $\alpha$  line widths, then using adiabatic theory to compute the density ratio; (2) measuring ion temperatures of several species having different charges and masses and applying collisionless theories of multi-ion shock heating (e.g., Lee et al. 1987; Lee & Wu 2000) to compute the compression ratio that is most consistent with the observations (for both methods, see Mancuso et al. 2002).

UVCS routinely obtains the densities, ionization states and elemental abundances in the pre-CME corona (e.g., Raymond et al. 2003). The densities obtained by UVCS

can be combined with Type II radio burst drift rates to obtain shock speeds. Upper limits on the coronal Alfvén speed above active regions were inferred from the derived shock speeds by requiring that the disturbances propagate at least as fast as the local characteristic speed (Mancuso et al. 2003). For a subset of events, the resulting shock speeds are in much better agreement with LASCO CME expansion rates than shock speeds based upon average coronal density profiles, although there are some uncertainties in the measured drift rates (Mancuso & Raymond 2004). The Alfvén and shock speeds can be inferred from detection of the shock arrival at different heights as determined by the timing of the increase in line widths of UV emission lines (e.g., Ciaravella et al. 2005). The angle between the shock front and the magnetic field requires the pre-shock field direction, which can be determined from streamer morphology. Severe elemental depletions are often observed in the closed field portions of streamers (Uzzo et al. 2004), providing an additional indicator of field topology. Another parameter potentially vital to the efficiency of shock acceleration is the density of suprathermal seed particles (e.g., Desai et al. 2003). While UVCS was not able to detect such particles, the improved sensitivity and instrumental profile characterization of next-generation instruments will make it possible to determine suprathermal particle densities out to  $\sim 6$  times the mean proton thermal speed (Cranmer 1998).

Although UVCS has proven the feasibility of detecting and characterizing CME shocks for several representative events, next-generation instrumentation can provide more extensive diagnostics and more complete spatial and temporal coverage. The empirical characterization of the coronal shock conditions and the ambient solar wind properties can then be used as inputs to: (1) 3D MHD models of the shock propagation through the heliosphere, and (2) multi-scale models of the SEP acceleration, transport, and energy spectrum synthesis (Zank et al. 2000; Li et al. 2003; Rice et al. 2003). Such constraints need to be applied in order to model specific events, such as the massive solar storms of Oct–Nov 2003. SEP acceleration and transport models can be tested for specific events by using spectroscopy and other remote-sensing diagnostics to constrain the initial parameters of the shock in the corona, then comparing with observed SEP energy spectra from, e.g., the Inner Heliospheric Sentinels. Iterative testing and refinement will ultimately result in a comprehensive validation of a predictive SEP model.

## 2.2. CME Current Sheets

Models of CMEs rely heavily on reconnection in current sheets, either trailing beneath the ejected magnetic flux rope or creating the flux rope in the first place (see Klimchuk 2001). Reconnection dumps large amounts of energy in the lower atmosphere of the Sun, creating intense heating, which accounts for the traditional flare ribbons and loops and for the current sheet containing hot plasma (Forbes et al. 1989; Švestka & Cliver 1992; Forbes & Acton 1996; Priest & Forbes 2002).

UVCS observations made it possible for the first time to allow us to carry out diagnostics of the plasma inside the current sheet (Ciaravella et al. 2000; Ko et al. 2003). A narrow feature was seen in [Fe XVIII] emission in the space between the post-flare loops and the CME core, indicating electron temperatures near  $6 \times 10^6$  K. Significant progress in studying the current sheet and the process of magnetic reconnection in the current sheet was made recently when the UV spectral data of the plasma inside the current sheet during two events on January 8, 2002 and on November 18, 2003 were obtained and analyzed (Ko et al. 2003; Lin et al. 2005). Both events developed a fast CME, a growing flare loop system, and a long current sheet that connects CME and flare loops. In one of these events, the pattern of the reconnection inflow near the current sheet was well recorded in H I Ly $\alpha$ . This allowed us to deduce the speed of the reconnection inflow directly and even to estimate the thickness of the current sheet. Also, it is possible to determine the magnetic field strength by using the observed speeds, densities, and temperatures to compute the kinetic and thermal energy densities in the reconnection region, then assume that this energy comes from the annihilation of an equal amount of magnetic energy just outside the current sheet (Ko et al. 2003). All of the parameters described above are required in order to put empirical constraints on the *reconnection rate* and electric field strength in the current sheet.

Such progress has very important theoretical consequences: for example, we are able to deduce the electrical resistivity (conductivity) in the current sheet, or in the reconnection region. Results obtained from UVCS and other remote-sensing instruments can provide the value of the electrical conductivity of the plasma inside the current sheet in an ongoing eruption for the first time since the impetus of applying reconnection theory to solar eruptions began six decades ago (Giovannelli 1946; and also see Priest & Forbes 2000).

With the knowledge of the dynamical process inside the current sheet, we are further able to investigate the particle acceleration taking place in the current sheet. A strong electric field is induced by magnetic reconnection in the current sheet. For a typical event, the electric field strength reaches about 5 V/cm (e.g., Wang et al. 2003; Qiu et al. 2004 for observations, and Martens & Kuin 1989; Forbes & Lin 2000; Lin 2002 for theories). An extremely high value of 50 V/cm was also reported (Xu et al. 2004). In principle, such a strong electric field is able to accelerate any charged particles. The current sheet is an assembly of waves and electric field, and accelerations can occur in various ways (see also Miller & Roberts 1995; Litvinenko 2000). We do not yet know exactly what happens in a real eruptive process, but the observations that a series of bright blobs flow successively out of the current sheet (e.g., Ko et al. 2003; Lin et al. 2005) replicate one of the main characteristics of magnetic reconnection inside the turbulent current sheet: the turbulent eddies or small magnetic islands inside the current sheet tend to merge into bigger ones before they leave the current sheet (Ambrosiano et al. 1988).

Further progress in understanding the above processes occurring in the current sheet depends on the accurate measurement of the thickness of the current sheet, plasma parameters in the current sheet (including electron and ion velocity distributions and densities), the speeds of reconnection inflow/outflow near the current sheet, as well as electric and magnetic fields in and around the current sheet. UV coronagraphic spectroscopy is uniquely suited to these requirements.

### 3. THE SOLAR WIND

UVCS has led to fundamentally new views of the *acceleration region* of the solar wind. By measuring emission lines formed both by collisional excitation and by the resonant scattering of solar-disk photons, UV spectroscopy provides a multi-faceted characterization of the kinetic properties of atoms, ions, and electrons (e.g., Withbroe et al. 1982; Cranmer 2002a). The Doppler-broadened shapes of emission lines are direct probes of line-of-sight (LOS) particle velocity distributions (i.e., essentially providing  $T_{\perp}$  when the off-limb magnetic field is  $\sim$ radial), and red/blue Doppler shifts reveal bulk flows along the LOS. Integrated intensities of resonantly scattered lines can be used to constrain the solar wind velocity and other details about the velocity distribution in the radial direction (e.g.,  $u_{\parallel}$  and  $T_{\parallel}$ ); this is the so-called “Doppler dimming/pumping” diagnostic (e.g., Noci et al. 1987). Intensities of collisionally dominated lines—especially when combined into an emission measure distribution—can constrain electron temperatures, densities, and elemental abundances in the coronal plasma. Even departures from Maxwellian and bi-Maxwellian velocity distributions are detectable with spectroscopic measurements having sufficient sensitivity and spectral resolution (e.g., Cranmer 2001).

In the high-speed solar wind, UVCS measured outflow speeds that were found to become supersonic much closer to the Sun than previously believed. In coronal holes, heavy ions (e.g.,  $O^{+5}$ ) were found to flow faster, to be heated hundreds of times more strongly than protons and electrons, and to have anisotropic temperatures with  $T_{\perp} > T_{\parallel}$  (Kohl et al. 1997, 1998, 1999; Cranmer et al. 1999). These unexpected results have rekindled theoretical efforts to understand the heating and acceleration of the fast wind in the extended corona (e.g., Tu & Marsch 1997; Leer et al. 1998; Axford et al. 1999; Hollweg 1999; Hollweg & Isenberg 2002; Marsch 2004).

The slow solar wind was found to flow mostly along the outer edges of bright streamers, near locations with measured abundance patterns matching those of the *in situ* slow wind (Strachan et al. 2002; Raymond et al. 1997). The closed-field “core” regions of streamers, though, exhibit heavy element abundances only 3 to 30% of those seen at 1 AU, indicating gravitational settling (e.g., Raymond 1999; Vásquez & Raymond 2005). UVCS observed the transition from a high-density collision-dominated plasma at low heights in streamers to a low-

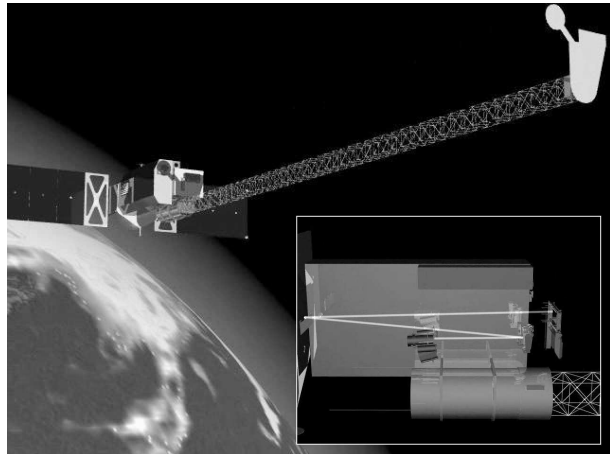


Figure 1. Spacecraft concept for advanced large-aperture coronagraphs. Inset shows a diagram of an Advanced UV Coronagraph Spectrometer.

density collisionless plasma at large heights, the latter exhibiting high ion temperatures and anisotropies that suggest similar physics as in the fast wind (Ko et al. 2002; Frazin et al. 2003).

If the kinetic properties of *additional ions* were to be measured in the extended corona (i.e., a wider sampling of charge/mass combinations) we could much better constrain the specific kinds of waves that are present as well as the specific collisionless damping modes (e.g., Cranmer 2002b). Measuring the *electron temperature* above  $\sim 1.5 R_{\odot}$  (never done directly before) would finally allow us to determine the bulk-plasma heating rate in different solar wind structures, thus putting the firmest ever constraints on models of why the slow [fast] speed wind is slow [fast] (e.g., Suess et al. 1999; Endeve et al. 2004; Cranmer, these proceedings). Measuring *non-Maxwellian velocity distributions* of electrons and positive ions would allow us to test specific models of MHD turbulence, cyclotron resonance, and velocity filtration. New capabilities such as these would be enabled by greater photon sensitivity, an expanded wavelength range, and the use of measurements that heretofore have only been utilized in a testing capacity (e.g., Thomson-scattered H I Ly $\alpha$  to obtain  $T_e$ ; the Hanle effect to obtain constraints on the magnetic field). These would then allow the relative contributions of different physical processes to the heating and acceleration of all solar wind plasma components to be determined directly.

### 4. IMPLEMENTATION

A mission capable of carrying out the required observations would include two instrument units: a large-aperture ultraviolet coronagraph spectrometer (see Fig. 1) and a large-aperture visible light coronagraph. A suitable design was developed during a MDEX Feasibility Study for a mission called ASCE. Remote external

occulters supported by a deployable boom provide much larger unvignetted apertures than are possible with conventional coronagraphs. These instruments provide major improvements in sensitivity, stray light rejection, spatial resolution, minimum observable height and ultraviolet wavelength range. New spectroscopic diagnostics for the electron velocity distribution, magnetic field, and parameters for a broad range of newly observable ions are implemented by these instruments. Unprecedented cadences are possible.

This work is supported by NASA under grants NNG-04GE77G, and NNG04GE84G to the Smithsonian Astrophysical Observatory.

## REFERENCES

- Ambrosiano, J., et al. 1988, JGR, 93, 14383
- Axford, W. I., et al. 1999, Space Sci. Rev., 87, 25
- Ciaravella, A., et al. 1997, ApJ, 491, L59
- Ciaravella, A., et al., 2000, ApJ, 529, 575
- Ciaravella, A., et al. 2002, ApJ, 575, 1116
- Ciaravella, A., et al. 2005, ApJ, 621, 1121
- Cranmer, S. R. 1998, ApJ, 508, 925
- Cranmer, S. R. 2001, JGR, 106, 24937
- Cranmer, S. R. 2002a, Space Sci. Rev., 101, 229
- Cranmer, S. R. 2002b, in SOHO-11: From Solar Min to Max, ESA SP-508, 361 (arXiv astro-ph/0209301)
- Cranmer, S. R., et al. 1999, ApJ, 511, 481
- Desai, M. I., et al. 2003, ApJ, 588, 1149
- Endeve, E., Holzer, T. E., Leer, E. 2004, ApJ, 603, 307
- Forbes, T. G., Acton, L. W. 1996, ApJ, 495, 330
- Forbes, T. G., et al. 1989, Solar Phys., 120, 285
- Frazin, R. A., et al. 2003, ApJ, 597, 1145
- Giovanelli, R. G., 1946, Nature, 158, 81
- Hollweg, J. V. 1999, JGR, 104, 505
- Hollweg, J. V., Isenberg, P. A. 2002, JGR, 107 (A7), 1147, doi:10.1029/2001JA000270
- Klimchuk, J. A. 2001, in Space Weather, ed. Song, P., Singer, H. J., Siscoe, G. L. (AGU: Washington, DC)
- Ko, Y.-K., et al. 2002, ApJ, 578, 979
- Ko, Y.-K., et al. 2003, ApJ, 594, 1068
- Kohl, J. L., et al. 1995, Solar Phys., 162, 313
- Kohl, J. L., et al. 1997, Solar Phys., 175, 613
- Kohl, J. L., et al. 1998, ApJ, 501, L127
- Kohl, J. L., et al. 1999, ApJ, 510, L59
- Lee, L. C. et al., 1987, JGR, 92, 13438
- Lee, L. C., Wu, B. H. 2000, ApJ, 535, 1014
- Leer, E., et al. 1998, in Cyclical Variability in Stellar Winds, ed. L. Kaper, A. Fullerton (Springer), 263
- Li, G., Zank, G. P., Rice, W. K. M. 2003, JGR, 108 (A2), 1082, doi:10.1029/2002JA009666
- Lin, J. 2002, Chinese J. Astron. Astrophys., 2, 539
- Lin, J., Forbes, T. G. 2000, JGR, 105, 2375
- Lin, J., Soon, W. 2004, New Astron., 9, 611
- Lin, J., et al. 2004, ApJ, 602, 422
- Lin, J., et al. 2005, ApJ, 622, 1251
- Litvinenko, Y. E. 2000, Solar Phys., 194, 327
- Mancuso, S., et al. 2002, A&A, 383, 267
- Mancuso, S., et al. 2003, A&A, 400, 347
- Mancuso, S., Raymond, J. C. 2004, A&A, 413, 363
- Marsch, E. 2004, in SOHO-15: Coronal Heating, ed. R. W. Walsh, J. Ireland, D. Danesy, B. Fleck, ESA SP-575, 186
- Martens, P. C. H., Kuin, N. P. M. 1989, Solar Phys., 122, 263
- Miller, J. A., Roberts, D. A. 1995, ApJ, 452, 912
- Noci, G., et al. 1987, ApJ, 315, 706
- Priest, E. R., Forbes, T. G. 2000, Magnetic Reconnection: MHD Theory and Applications (Cambridge Univ. Press, Cambridge), ch. 8
- Priest, E. R., Forbes, T. G., 2002, A&A Rev., 10, 313
- Qiu, J., et al. 2004, ApJ, 604, 900
- Raymond, J. C. 1999, Space Sci. Rev., 87, 55
- Raymond, J. C. 2002, in SOHO-11: From Solar Min to Max, ESA SP-508, 421
- Raymond, J. C., et al. 1997, Solar Phys., 175, 645
- Raymond, J. C., et al. 2000, GRL, 27, 1439
- Raymond, J. C., et al. 2003, ApJ, 597, 1106
- Reames, D. V. 1995, Rev. Geophys. Suppl., 33, 585
- Reames, D. V. 1999, Space Sci. Rev., 90, 413
- Rice, W. K. M., Zank, G. P., Li, G. 2003, JGR, 108 (A10), 1369, doi:10.1029/2002JA009756
- Speiser, T. W. 1965, JGR, 70, 4219
- Strachan, L., et al. 2002, ApJ, 571, 1008
- Suess, S. T., et al. 1999, JGR, 104, 4697
- Švestka, Z., Cliver, E. W. 1992, in Eruptive Solar Flares, ed. Z. Švestka, B. V. Jackson, M. E. Machado (New York: Springer-Verlag), pp. 1–14
- Tu, C.-Y., Marsch, E. 1997, Solar Phys., 171, 363
- Uzzo, M., Ko, Y.-K., Raymond, J. C. 2004, ApJ, 603, 760
- Vásquez, A. M., Raymond, J. C. 2005, ApJ, 619, 1132
- Vršnak et al. 2002, A&A, 396, 673
- Wang, H., et al. 2003, ApJ, 593, 564
- Withbroe, G. L., et al. 1982, Space Sci. Rev., 33, 17
- Xu, Y., et al., 2004, ApJ, 607, L131
- Zank, G. P., et al. 2000, JGR, 105, 25079